Charge-exchange reaction with light neutron-rich beams

M.D. Cortina-Gil, A. Pakou, N. Alamanos, W. Mittig, P. Roussel-Chomaz, F. Auger, J. Barrette, Y. Blumenfeld, J.M. Casandjian, M. Chartier, et al.

GANIL

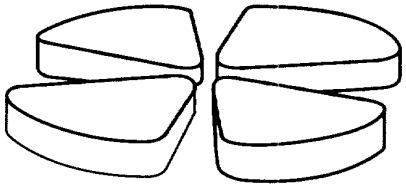

Submitted in Physics Letters B

Charge-exchange reaction induced by ^{6}He and nuclear densities

M.D. Cortina-Gil[a,1], A. Pakou[b,h], N. Alamanos[b], W. Mittig[a], P. Roussel-Chomaz[a], F. Auger[b], J. Barrette[c], Y. Blumenfeld[e], J. M. Casandjian[a,2], M. Chartier[a,3], F. Dietrich[d], V. Fekou-Youmbi[b,4], B. Fernandez[b], N. Frascaria[e], A. Gillibert[b], H . Laurent[b], A. Lepine-Szily[f], N. Orr[g], V. Pascalon[e], J. A. Scarpaci[e], J. L. Sida[b], T. Suomijarvi[e]

GANIL P 98 19

Charge-exchange reaction induced by ^{6}He and nuclear densities

M.D. Cortina-Gil[a,1], A. Pakou[b,h], N. Alamanos[b], W. Mittig[a], P. Roussel-Chomaz[a], F. Auger[b], J. Barrette[c], Y. Blumenfeld[e], J. M. Casandjian[a,2], M. Chartier[a,3], F. Dietrich[d], V. Fekou-Youmbi[b,4], B. Fernandez[b], N. Frascaria[e], A. Gillibert[b], H . Laurent[b], A. Lepine-Szily[f], N. Orr[g], V. Pascalon[e], J. A. Scarpaci[e], J. L. Sida[b], T. Suomijarvi[e]

[a]GANIL(DSM/CEA, IN2P3/CNRS), BP 5027,14021 Caen Cedex, France
[b]CEA/DSM/DAPNIA/SPhN Saclay, 91191 Gif-sur-Yvette Cedex, France
[c]Foster Radiation Lab. Mc Gill University, Montreal, Canada H3A 2T8
[d]Lawrence Livermore National Laboratory, Livermore, California 94550
[e]IPN, IN2P3/CNRS 91406 Orsay Cedex, France
[f]IFUSP, DFN, C. P 66318, 05315-970, Sao Paulo, S. P Brasil
[g]LPC- ISMRA, Blvd du Maréchal Juin, 1405 Caen, France
[h]Department of Physics , The University of Ioannina, Greece

Abstract

The charge exchange reaction p(^{6}He, ^{6}Li)n was studied in reverse kinematics with a secondary ^{6}He beam at 41.6 MeV /nucleon. The transition connecting the ground state of ^{6}He to its isobaric analog state in ^{6}Li has been measured and analyzed in the context of a microscopic calculation. The angular distribution is shown to be sensitive to the nuclear interaction potential and to the radii of the density distribution of ^{6}He. It is shown that only a coherent microscopic analysis may disentangle the different contributions.

[1] Present address: GSI, Postfach 110552, D-64220 Darmstadt, Germany
[2]Present address: Nucl. Phys. Lab., Univ. of Washington, Seattle, WA 98195, USA
[3]Present address: NSCL, Michigan State University, East Lansing, MI 48824, USA
[4]Present address: Oregon State University, 100 Radiation Center, Corvallis, OR 97331-5903, USA

1. Introduction

Nucleon-nucleus elastic scattering and charge exchange reactions have been widely studied in the past with stable targets and provided valuable information on nuclear properties such as the nucleon-nucleus interaction, energy levels or transition matrix elements [1-2]. It was shown by Lane that the inclusion of the isospin term in the optical potential has the effect of mixing all the channels with the same total isospin [3]. In this way, the charge-exchange reaction (p,n) connecting two isobaric analog states is related to the elastic scattering reaction because the structure of the target and the residual nucleus are essentially the same, differing only in the projection of the isospin. Therefore, a consistent description of the (p,p) and (p,n) angular distributions could provide information on the isoscalar and isovector part of the nucleon-nucleon interaction and could also, in principle, probe differences between the proton and neutron density distributions [4]. Nowadays, the availability of intense secondary beam facilities allows to extend these studies to unstable nuclei where very large differences between proton and neutron density distributions are expected and to test our understanding of the nuclear properties far from the valley of stability.

We have studied the p(^{6}He,^{6}Li)n reaction populating two states of ^{6}Li : the ground state via a Gamow-Teller transition (GT) and the 3.56 MeV excited state, which is the isobaric analog state (IAS) of the ^{6}He ground state and is populated via a Fermi transition. Like the ^{6}He ground state, the IAS of ^{6}Li is predicted theoretically to be a halo state [5]. Therefore this reaction provides the opportunity to study simultaneously transitions connecting a halo state to either a standard or another halo state.

The ratio of the cross sections at zero degree for the two transitions is directly connected to the relative strength of the two components of the isospin exchange interaction $V_{\sigma\tau}$ and V_{τ} and was investigated in a previous publication [6]. It was found to be compatible with existing systematics for stable T=1 nuclei and did not reveal any signature of the halo structure of the ^{6}He ground state. These results were confirmed by recent measurements which have also shown that the ratio of the $V_{\sigma\tau}$ and V_{τ} interactions is compatible with that expected from (p,n) systematics and β decay [7,8,9].

In this work we present a detailed microscopic analysis for the IAS transition, for which the form factor is directly related to the difference between the neutron and proton density distributions and therefore is expected to be sensitive to the halo structure.

2. Experimental Details and Results

A detailed description of our experimental method was given previously [6,10]. We give here only a short summary of the experimental details pertinent in this work.

The secondary beam was produced by fragmentation of a 75 MeV/nucleon ^{13}C beam delivered by the GANIL accelerator on a 1155 mg/cm^2 carbon production target, located between the two superconducting solenoids of the SISSI device [11]. The secondary beam was analyzed by the alpha spectrometer with a magnetic rigidity set at 2.82 Tm which corresponds to an average energy of 41.6 MeV/nucleon for the ^{6}He ions. In these conditions, the total intensity of the secondary beams was of the order of 10^7pps. The intensity of the neutron-rich nucleus ^{6}He, corresponded to a few percent of the total intensity.

A momentum spectrum obtained for the reaction p(^{6}He,^{6}Li)n at θ_{lab}=1° is shown in Fig. 1. The narrow peak at Q=0 corresponds to the stripping in the target of the $^6Li^{2+}$ secondary beam. This peak provides a direct measurement of the angular width of the secondary beam which for the (p,n) measurements was around 1°. The width of the peak also provides a measurement of the energy spread of the beam due to target inhomogenities and energy straggling. The other peaks correspond from right to left to the (p,n) reaction populating the ground state and IAS of ^{6}Li, respectively. The reaction peaks are broadened due to kinematics effects and to the difference in energy loss in the target between ^{6}He and ^{6}Li. The latter peak is further broadened due to the in flight γ-decay of ^{6}Li.

The angular distributions corresponding to both transitions studied here are shown in Fig.2. Because we could not determine the absolute ^{6}He beam intensity, absolute cross sections were obtained by comparing our (GT) transition data with previously reported values [9] for the inverse ^{6}Li(n,p)^{6}He reaction, for which the cross section is directly connected by the reciprocity theorem with our data, as long as spin corrections are applied [6].

The same reactions have been studied at 93 MeV/nucleon in Ref. [7] but no absolute cross sections were given. When plotted as a function of the transfer momentum, the shape of the angular distribution for the GT transition is in agreement with our data. The fact that the relative yield of the IAS transition in Ref. [7] is much weaker than reported here can be explained by the higher incident energy. However, the angular

distribution for this transition is flatter than in our data. This disagreement may be due to the poorer separation in Ref. [7] between the IAS state and the background.

3. Analysis and Discussion

As mentioned above, the inclusion of an isospin term U_1 in the optical potential U which is responsible for elastic scattering,

$$U = U_0 + \frac{4}{A}\bar{t}.\bar{T}U_1$$

leads in a natural way to the excitation of IAS states in (p,n) reactions. In this relation $\bar{t}$ and $\bar{T}$ refer to the isobaric spins of projectile and target, respectively.

In this model the isoscalar part of the optical potential, U_0 is proportional to the isoscalar density of the nucleus ($\rho_n(r)+\rho_p(r)$), where ρ_n and ρ_p are the neutron and proton density distributions respectively while the isovector part of the optical potential, U_1 is related to the isovector density of the nucleus ($\rho_n(r)-\rho_p(r)$). Charge exchange reactions between analog states are mediated by the second term of the optical potential U and therefore provide information on the difference between the neutron and proton density distributions in a nucleus. This type of calculation seems to reproduce reasonably well the (p,n) charge exchange reaction to isobaric-analog states of light nuclei [12].

In the present work the optical and coupling potentials were calculated by a folding model using the microscopic JLM nuclear matter optical potential [13] based on Reid's hard core interaction [14]. The JLM potentials have proven to yield quite satisfactory results for the light nuclei. Proton and neutron elastic scattering from ^{6}Li, ^{7}Li, ^{12}C, ^{13}C, ^{14}C, and ^{16}O in the range 20-50 MeV can be reproduced successfully provided the imaginary part of the potential is renormalized by a factor λ_w=0.8, [12,15-17].

A frequently employed procedure for stable nuclei is to extract the proton distribution, ρ_p from electron scattering data and then to adopt for neutrons a distribution according, for example, to the relationship $\rho_n=(N/Z)\rho_p$. However in the present case, where we have to deal with the exotic nucleus ^{6}He, such a simple procedure is no longer valid. To analyze the data we have used an optical model potential, obtained by using the standard JLM interaction for stable nuclei (λ_v=1, λ_w=0.8) [17] with neutron and proton densities obtained by Hartree-Fock calculations [18].

These calculations (solid lines in Figs. 3a and 3b) failed to reproduce the experimental data, both in shape and absolute normalization. This is consistent with the conclusions of Ref. [10] where it is shown that the elastic scattering angular distribution p(^{6}He,^{6}He)p, at the same energy is not well reproduced by standard normalization parameters. It was suggested in that work that a good fit could be obtained by adjusting either the real part or the imaginary part of the optical potential. The effect of the normalization of the real and imaginary part of the entrance channel optical potential for the present (p,n) data is shown in Figs 3a and 3b, respectively. Fig. 3a shows that renormalizing the real potential has little effect on the calculated angular distribution. However, as shown in Fig. 3b a reasonable description of the data is obtained if one renormalized the imaginary potential to a value λ_w=1.8, a value that also gives the best fit to the elastic angular distribution [10]. In the calculations, the interaction is treated consistently in the sense that the same normalizations (λ_v=1.0, λ_w=1.8) are used for the entrance and exit optical potentials as well as for the (p,n) form factor.

This need to increase the absorptive part of the JLM isovector potential is consistent with the analysis of Ref. [17]. In this work it is concluded from an analysis of the charge exchange reaction on ^{208}Pb that in the JLM potential the ratio U_1/U_0 is too small by a factor of roughly 2. A larger ratio between the isovector and isoscalar potential is also consistent with other empirical parametrizations of the nucleon-nucleus potential deduced from analysis of nucleon elastic scattering [19-22]. A deeper understanding of the present results will need further investigations of the JLM isovector potential in both light and heavy nuclei.

In Fig. 3c we have explored the sensitivity of the calculations to the assumed nucleon density distributions. Proton and neutron density distributions used in these calculations are shown in Fig. 4. In all these JLM calculations we have assumed constant real and imaginary normalizing parameters λ_v=1 and λ_w=1.8, respectively. The dashed line corresponds to the dashed line in Fig. 3b and corresponds to the Hartree-Fock density distributions [18]. The Hartree-Fock calculations predict that the ^{6}He neutron distribution has a halo structure and a r.m.s. radius R_n=2.36 fm much larger than the proton distribution R_p=1.90 fm. The dot-dashed line assumed that the neutrons have the same density distribution as the protons (ρ_n= (N/Z) ρ_p). The calculation assuming such a non halo neutron distribution is in strong disagreement with the experimental results and underpredicts the measured cross sections.

The other curves assume that the proton and neutron nucleon distributions are of gaussian shape. The dotted line is for distributions with root mean square radii corresponding to the previous Hartree-Fock density distributions while the solid line corresponds to root mean square radii obtained from a Glauber analysis of recent p(^{6}He,^{6}He)p elastic scattering data obtained at high energy [23] (R_p=1.88±0.12 fm, R_n=2.48±0.11 fm). These distributions also give results close to the experimental values. It is interesting to note the sensitivity of the (p,n) cross sections not only to different radii but also to different shapes of the distribution. An increase of about 0.1 fm in the neutron r.m.s. radius is reflected by an increase of 20% of the cross section at forward angles. Furthermore, density distributions having the same r.m.s. radii, but differing only in their tails (halo or not) give a difference of 20% at forward angles. This contrasts with the elastic scattering angular distribution which shows little sensitivity to the exact shape of the density distribution. It should be reminded that the neutron r.m.s. radius extracted from the H.F. calculations is smaller than the results deduced from high energy elastic scattering on a proton target [23], and from the interaction cross section measurements [24]. The fact that the corresponding calculated cross sections are slightly smaller than the data corroborates these results. The present analysis assumed that the IAS in ^{6}Li has a similar shape as the ^{6}He. However, for light exotic nuclei it may be needed to take explicitly into account the difference in structure between the entrance and exit channel.

In summary, angular distributions for the reaction connecting the ground state of ^{6}He and the ground and excited states of ^{6}Li have been obtained. A consistent description of the angular distribution for the transition to the IAS in ^{6}Li is obtained using the JLM empirical nucleon-nucleus potential. To fit the data for both elastic scattering and charge exchange reaction leading to the IAS of ^{6}He requires, however, a significant increase of the imaginary part of the JLM potential. Furthermore, the analysis of the angular distribution for the charge exchange reaction shows evidence that the r.m.s. radius of the neutrons in ^{6}He is much larger than that of the protons. Therefore the observation made previously that the value of the cross section at zero degrees for charge exchange reactions is consistent with the systematic behavior established for stable T=1 nuclei [6], seems to be the result of a compensation between the influence of the increased imaginary part of the interaction potential and the increase of the r.m.s. radius of the neutron density distribution in a halo nucleus. Only a coherent microscopic analysis, as presented here, may disentangle these contributions. This shows that the study of charge exchange reactions may be a very valuable tool to investigate the evolution of the isoscalar and isovector part of the nucleon-nucleus interaction far from the valley of stability and also to obtain complementary information on the nucleon density distributions.

REFERENCES

[1] G. R. Satchler and W. G. Love, Phys. Rep . 55 (1979) 183.

[2] N. Alamanos and P. Roussel-Chomaz, Ann. Phys. Fr. 21 (1996) 601 and references therein

[3] A.M. Lane, Nucl. Phys. 35 (1962) 676

[4] C.J. Batty et al., Advances in Nuclear Physics, Vol. 19, 1 (1989)

[5] K. Arai et al, Phys. Rev. C51 (1995) 2488.

[6] M. D. Cortina-Gil et al., Phys. Lett. B 371 (1996) 14.

[7] J. A. Brown et al., Phys. Rev. C 54 (1996) R2105.

[8] T. Teranishi et al., Phys. Lett. B 407 (1997) 110

[9] D. Pocanic et al., Can. J. Phys.65 (1987) 687, and
J. Rapaport et al., Phys. Rev. C41 (1990) 1920.

[10] M. D. Cortina-Gil et al., Phys. Lett. B. 401 (1997) 9, and
J.S. Al-Khalili et al., Phys. Lett. B 378(1996)45.

[11] W. Mittig, Nucl. Phys. News 1 (1990) 30. and
A. Joubert et al.,1991 Particle Accelerator Conference IEEE vol. 1 (1991) 594 ;

[12] F. Petrovich et al., Nucl. Phys. A563 (1993) 387.

[13] J.-P. Jeukenne, A. Lejeune and C. Mahaux, Phys. Rev. C 10(1974)1391 ; Phys. Rev. 15 (1977) 10 ; Phys. Rev. C16 (1977) 80.

[14] R. V. Reid, Ann. Phys. 50 (1968) 411.

[15] J.S. Petler et al., Phys. Rev. C32 (1985) 673.

[16] S. Mellema et al Phys.Rev. C 28 (1983) 2267.

[17] F. S. Dietrich and Petrovich, Proc. Conf. On Neutron-Nucleus Collisions- A probe of Nuclear Structure, ed. J. Rapaport et al., eds., AIP Conf. Proc. No. 124 (AIP, New York, 1985) p. 90.

[18] H. Sagawa, Phys. Lett B286 (1992) 315.

[19] F. D. Becchetti and G.W. Greenlees, Phys. Rev. 182 (1969) 1190.

[20] Patterson et al. Nucl. Phys. A263 (1976) 261.

[21] S. Austin, Proc. Conf. The (p,n) Reaction and the Nucleon-Nucleon Force, eds., C.D. Goodman et al. Plenum Press, 1980, page 203.

[22] R. L. Varner et al., Phys. Rep. 201 (1991) 57.

[23] G. D. Alkhazov et al. Phys. Rev. Lett. 78 (1997) 2313.

[24] I. Tanihata et al, Phys. Lett. B206 (1988) 592

FIGURE CAPTIONS

Fig. 1 : Momentum spectrum for the p(^{6}He, ^{6}Li)n charge exchange reaction.

Fig. 2 : Angular distributions for the p(^{6}He, ^{6}Li$_{g.s}$)n and the p(^{6}He, ^{6}Li$_{IAS}$)n reactions.

Fig. 3 : Comparison of the present experimental (p,n) results with : a) JLM calculations adopting different normalisation factors for the real part of the potential, λ_v, the normalisation factor for the imaginary part, λ_w, being fixed at 0.8, b) JLM calculations adopting different normalisation factors for the imaginary part of the potential, λ_w, the normalisation factor for the real part, λ_v, being fixed at 1.0, c) JLM calculations (λ_V=1, λ_W=1.8) assuming different density distributions, see text for more details.

Fig. 4 : Proton and neutron density distributions used in the JLM calculations. The dashed line corresponds to the Hartree Fock neutron density distribution [18], and the dotted line to a neutron density distribution of Gaussian shape and with a r.m.s. radius equal to the previous Hartree Fock density distribution. The solid line represents also a gaussian density distribution with a the r.m.s. radius obtained from high energy proton elastic scattering. The dot-dashed line is the neutron density distribution obtained assuming that the neutron density distribution has similar shape than the protons and that (ρ_n= (N/Z) ρ_p). The thin solid line corresponds to the proton Hartree Fock density distribution. The proton density distribution calculated assuming a Gaussian shape is very close to this thin solid line.

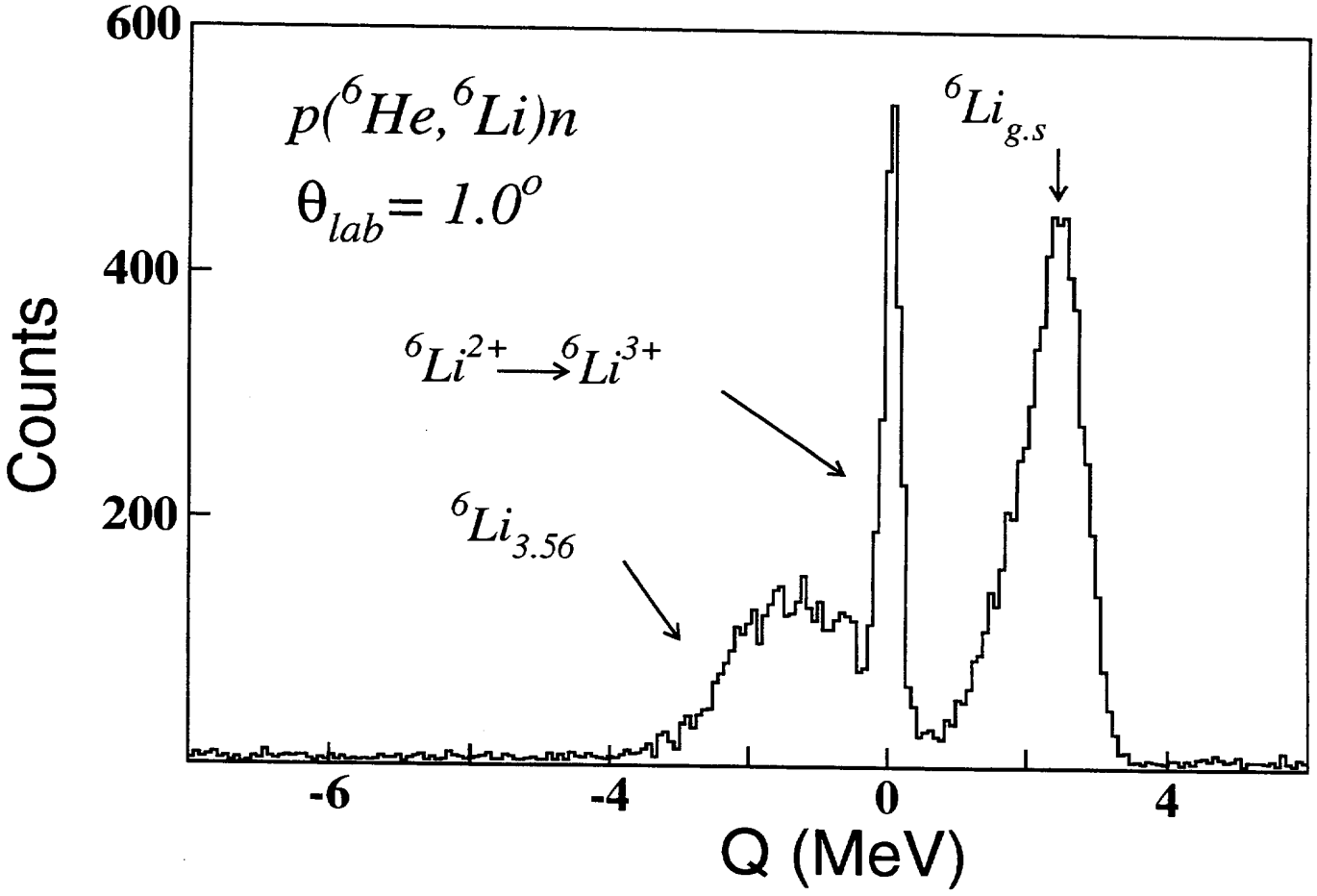
600
400
200
Counts
$p(^6He,^6Li)n$
$\theta_{lab}= 1.0^o$
$^6Li_{g.s}$
$^6Li^{2+} \longrightarrow ^6Li^{3+}$
$^6Li_{3.56}$
-6
-4
0
4
Q (MeV)

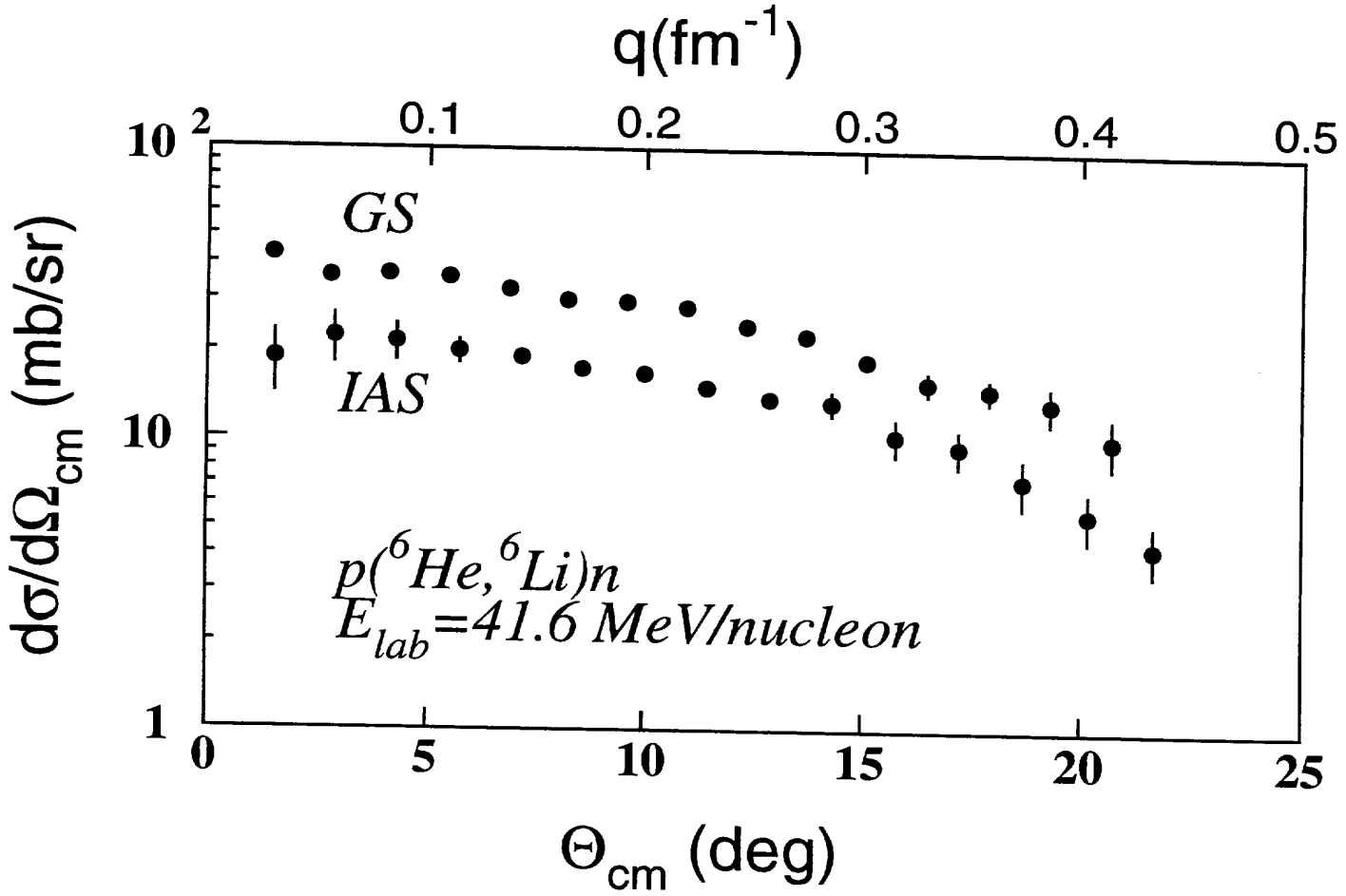
q(fm^{-1})
0.1
0.2
0.3
0.4
0.5
10^2
10
1
GS
IAS
$p(^6He,^6Li)n$
E_{lab}=41.6 MeV/nucleon
dσ/dΩ$_{cm}$ (mb/sr)
0
5
10
15
20
25
Θ$_{cm}$ (deg)

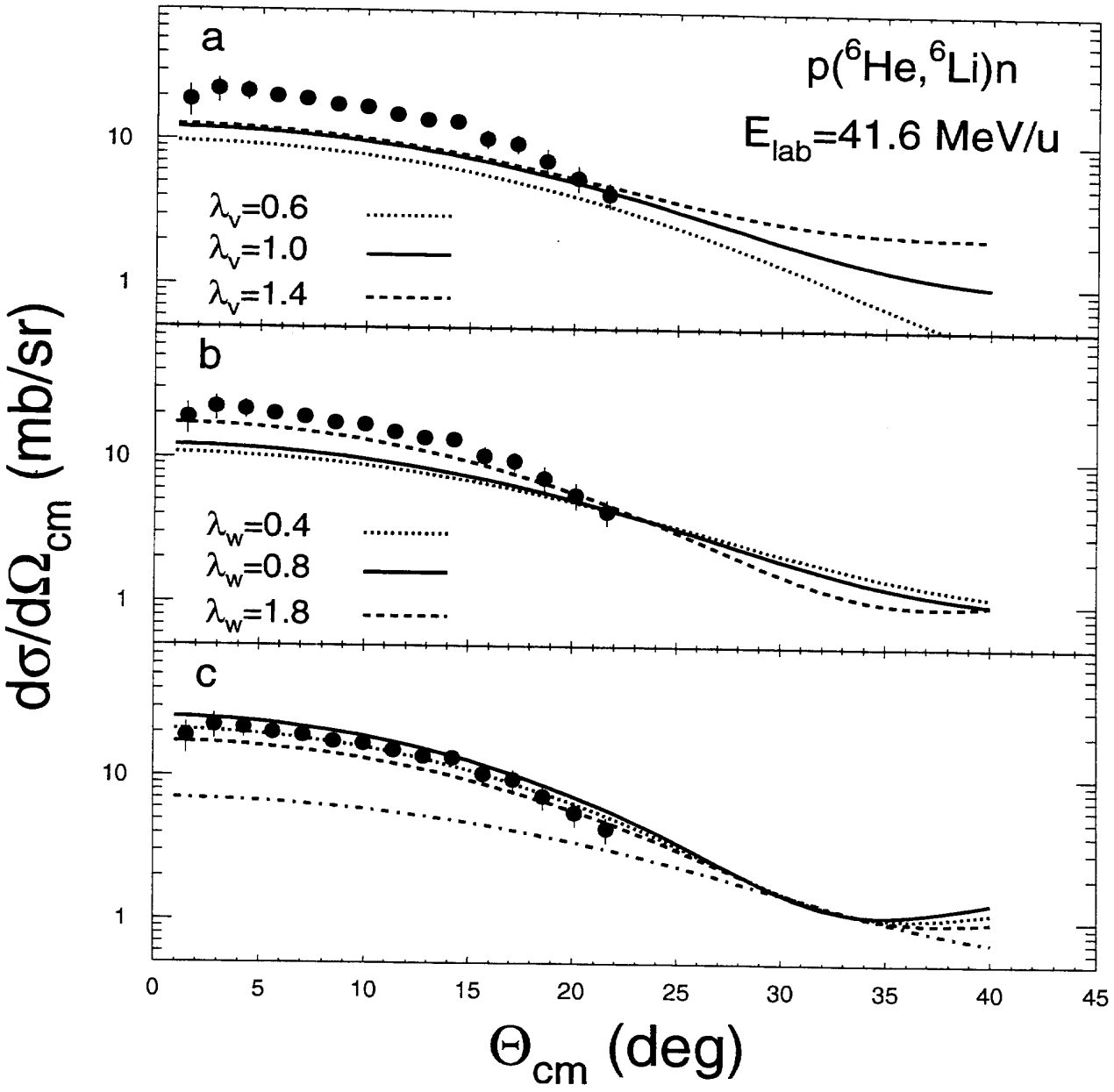
a
p(6He,6Li)n
Elab=41.6 MeV/u
λv=0.6
λv=1.0
λv=1.4
b
λw=0.4
λw=0.8
λw=1.8
c
10
1
dσ/dΩcm (mb/sr)
0
5
10
15
20
25
30
35
40
45
Θcm (deg)

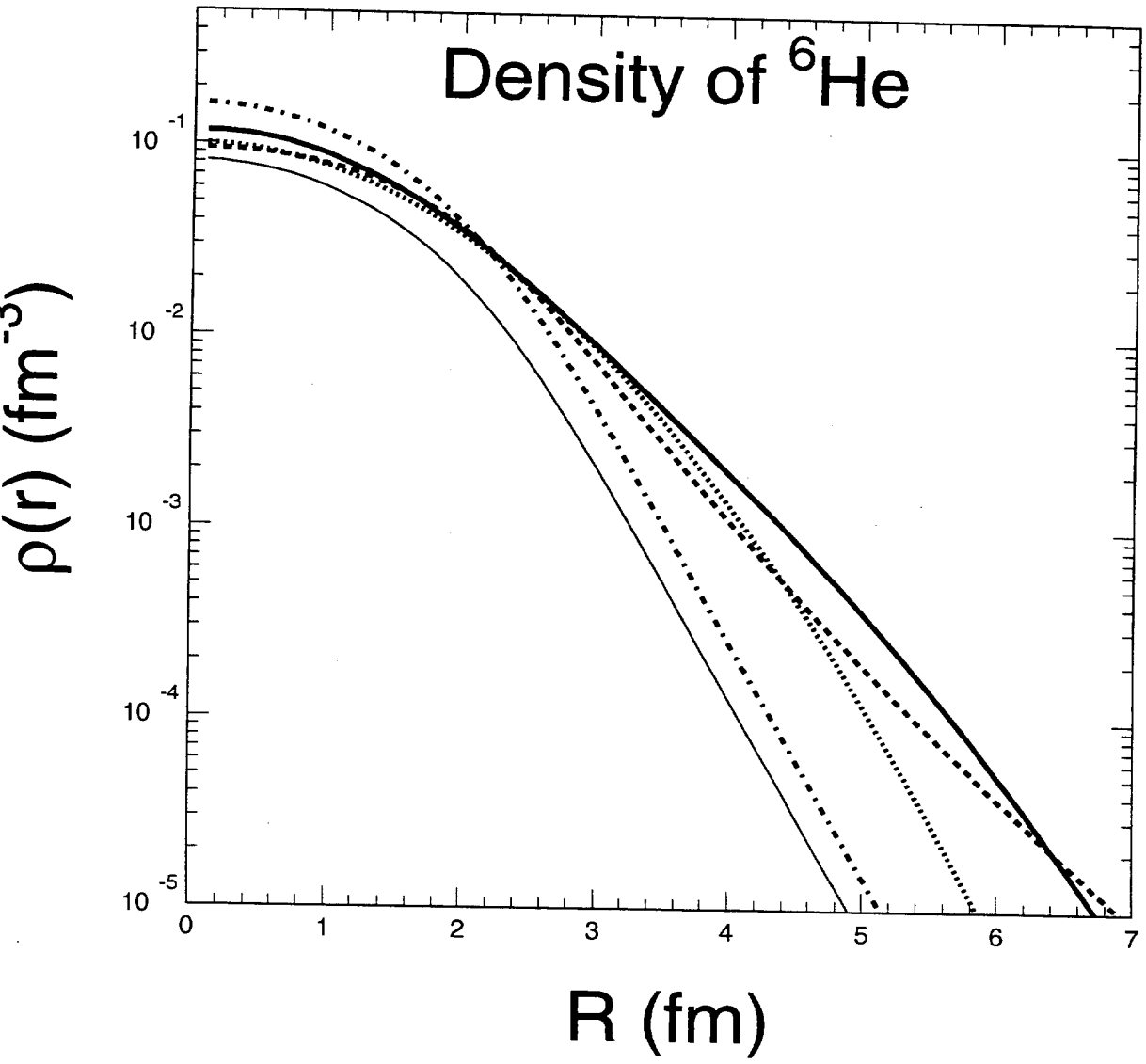
Density of ^{6}He
$\rho(r)$ (fm^{-3})
10^{-1}
10^{-2}
10^{-3}
10^{-4}
10^{-5}
0
1
2
3
4
5
6
7
R (fm)